



Numerical and acoustic investigation of cavitation phenomena in centrifugal hydraulic pumps

Saba A. Othman, Hashim A. Hussien, Abduljabbar O. Hanfesh

Online Publication Date: 30 November 2025

URL: <http://www.jresm.org/archive/resm2025-1249ic1012rs.html>

DOI: <http://dx.doi.org/10.17515/resm2025-1249ic1012rs>

Journal Abbreviation: *Res. Eng. Struct. Mater.*

To cite this article

Othman S A, Hussien H A, Hanfesh A O. Numerical and acoustic investigation of cavitation phenomena in centrifugal hydraulic pumps. *Res. Eng. Struct. Mater.*, 2026; 12(2): 845-858.

Disclaimer

All the opinions and statements expressed in the papers are on the responsibility of author(s) and are not to be regarded as those of the journal of Research on Engineering Structures and Materials (RESM) organization or related parties. The publishers make no warranty, explicit or implied, or make any representation with respect to the contents of any article will be complete or accurate or up to date. The accuracy of any instructions, equations, or other information should be independently verified. The publisher and related parties shall not be liable for any loss, actions, claims, proceedings, demand or costs or damages whatsoever or howsoever caused arising directly or indirectly in connection with use of the information given in the journal or related means.



Published articles are freely available to users under the terms of Creative Commons Attribution - NonCommercial 4.0 International Public License, as currently displayed at [here](#) (the "CC BY - NC").

Numerical and acoustic investigation of cavitation phenomena in centrifugal hydraulic pumps

Saba A. Othman ^{*,a}, Hashim A. Hussien ^b, Abduljabbar O. Hanfesh ^c

Electromechanical Engineering Department University of Technology-Iraq, Baghdad, Iraq

Article Info

Abstract

Article History:

Received 12 Oct 2025

Accepted 24 Nov 2025

Keywords:

Acoustic technique;
Cavitation;
Centrifugal pump;
Turbulent kinetic energy;
Hydraulic oil;
CFX;
Vapor volume fraction

Cavitation significantly reduces the performance and efficiency of centrifugal pumps. This study investigates cavitation behavior in a CRT 100-BR centrifugal pump using ISO 22 hydraulic oil produced locally at the Dora Refinery, Iraq, through a combination of numerical simulations (ANSYS CFX) and acoustic signal analysis. The pump operated at 6 bar, 2800 rpm, and 280 L/min. Acoustic signals recorded by a microphone were analyzed in MATLAB using mean, RMS, and peak amplitude indicators, revealing that peak amplitude values were approximately 42.86% higher than RMS, effectively detecting cavitation onset. Numerical simulations evaluated turbulent kinetic energy and vapor volume fraction at flow rates from 50 to 300 L/min, showing a 45% increase in vapor fraction and a 65% rise in turbulence energy when the flow increased from 200 to 300 L/min. These results demonstrate that integrating CFD modeling of turbulence and vapor fraction with acoustic analysis provides a reliable and efficient method for cavitation detection and pump condition monitoring.

© 2026 MIM Research Group. All rights reserved.

1. Introduction

Centrifugal pumps are hydrodynamic devices that utilize a revolving impeller to convey energy from the motor to the fluid. The energy transfer occurs via the impeller blades, which augment both the pressure and kinetic energy of the fluid at the impeller's output. Various faults may occur during actual operation. [1]. Cavitation often denotes the formation of cavities and the ensuing dynamic behaviors that occur when a liquid experiences a significant pressure reduction [2]. Cavitation is an unavoidable complicated process of multiphase flow involving phase transition below the liquid's vapor pressure at the operational temperature. A substantial quantity of bubbles is generated, which will implode once the liquid enters the high-pressure region. The mechanism of cavitation remains incompletely understood because of its stochastic nature and multiphase properties. Upon the occurrence of cavitation, the energy transfer between the impeller and the fluid is compromised, resulting in a decline of the head-flow rate curve, while the surfaces of the flow passage components experience significant wear and corrosion. Also, it will cause noise in pump body [3].

Acoustic monitoring has attracted increasing attention in recent years, such as Cernetic et al. [4] examined noise phenomena within the audible frequency range associated with cavitation in centrifugal pumps. They employed a dual-channel signal analyzer and two microphones with a frequency range of 100 Hz to 10 kHz for their investigation. The noise escalates prior to the 3% head drop, nevertheless the apex of the loudness is situated in proximity to the Critical Net Positive Suction Head (NPSH). The escalation of noise resulted from the formation and proliferation of cavitation bubbles that intensify flow turbulence, obstructing the flow channel. Moreover, vibrations resulting from unstable cavitation within the pump may exacerbate noise levels. S.

*Corresponding author: eme.22.47@grad.uotechnology.edu.iq

^aorcid.org/0009-0003-8109-6453; ^borcid.org/0000-0003-4036-3853; ^corcid.org/0000-0001-5345-1794

DOI: <http://dx.doi.org/10.17515/resm2025-1249ic1012rs>

Res. Eng. Struct. Mat. Vol. 12 Iss. 2 (2026) 845-857

Farokhzad and H. Ahmadi [5] developed a cavitation prediction system utilizing acoustic inputs and a multilayer perpendicular (MLP) neural network. This approach shown efficiency and reliability in frequency analysis under stable circumstances and consistent velocity. Hosien et al. [6] executed an empirical study to evaluate the efficacy of acoustic methods in identifying the start of cavitation in hydraulic systems. The findings indicated that cavitation produces acoustic signals within the frequency spectrum of 31.5 Hz to 31.5 kHz, which were distinctly captured through a transparent window in the water conduit. The results validated a robust association between acoustic signals and visual observations, indicating that acoustic measurement can serve as an effective and dependable method for ascertaining cavitation start. Dong et al. [7] presented an approach based on variations in vibration patterns and noise levels throughout the system's operation. The signals produced by cavitation were most prominent during the initiation of the phenomena, rendering this approach appropriate for application with big pumps.

Ranade and Sarvothaman [8] examined the application of acoustic data, gathered using a standard cell phone, to ascertain the initiation and magnitude of hydrodynamic cavitation. Acoustic emissions from vortex-based cavitation devices were documented at different pressure reductions (0–390 kPa). The 'Audio' and 'DSP' toolboxes in MATLAB were utilized to analyze the data and extract acoustic characteristics. Three distinct tendencies concerning flow rate and pressure decrease were identified. These patterns unequivocally signified the commencement of cavitation, particularly within the range of 50–80 kPa. A characteristic termed “flatness” has shown a strong correlation with cavitation levels and device efficacy. The research indicated that this methodology is suitable for real-time cavitation detection and confirmed its universal applicability across various cavitation systems. Ramadan et al. [9] identified cavitation within the centrifugal pump utilizing vibration and acoustic methodologies. This was accomplished by examining the acoustic waves in both temporal and frequency domains. Cavitation was examined by several statistical characteristics during temporal domain analysis (TDA). The fast Fourier transform (FFT) technique was employed for frequency domain analysis (FDA). Karagiovanidis et al. [10] presented a set of early methods for detecting cavitation in centrifugal irrigation pumps, based on vibration and acoustic signal analysis. They developed a low-cost data collection system and evaluated multiple computational algorithms. A smartphone-based accelerometer was used to collect vibration data, and the signals were then compared under different operating conditions. Stephen, C et al. [11] improved the Deviation from Normal Distribution (DND) method for cavitation detection using vibration signals. By comparing the original DND calculation with a baseline-data approach through probability density functions and normal probability plots, the results showed that the baseline method provided clearer and more sensitive indication of cavitation, enabling the definition of practical alarm limits. The improved technique was validated at different operating speeds and was found to be reliable, responsive, and independent of speed. Rahma et al. [12] Determined the four typical cavitation levels for pump type (CEA 210/2) operated on water. With the use of time-domain analytic tools, record the acoustic waves using a hydrophone. The result indicated that the low-frequency range of acoustic signals is highly effective for early cavitation detection. Ni, Chen et al. [13] investigated cavitation in a single-blade centrifugal pump through combined numerical and experimental vibration/noise analysis. Using time-frequency features, energy entropy, and vibration acceleration level, the results showed that cavitation introduces intermittent high-frequency shocks and increases dominant vibration components, while noise spectra exhibited reduced blade-passing frequency and amplified low-frequency content. The study confirmed clear quantitative links between cavitation severity and changes in vibration and acoustic behavior, supporting its use for cavitation monitoring in impurity-laden pump flows. Wang, D. et al. [14] used hydrophone-based acoustic measurements at the pump inlet and outlet to detect cavitation. Noise levels increased with flow rate, and decreasing NPSHa caused a sharp inlet noise drop and an initial outlet noise rise, allowing earlier cavitation detection. Dominant spectral components were shaft and blade frequencies and their harmonics, and changes in these acoustic features proved effective for predicting cavitation onset.

Previous studies on cavitation in centrifugal pumps have typically relied on single-method approaches or idealized water-based simulations that do not fully reflect real operating environments. In contrast, the present study integrates high-fidelity ANSYS CFX simulations with

experimental acoustic measurements conducted under industrial conditions using locally produced Iraqi ISO 22 hydraulic oil (Daura Refinery) in a CRT 100-BR centrifugal pump. Time-domain statistical indicators, alongside CFX-predicted vapor volume fraction and turbulent kinetic energy, were analyzed to establish a direct correlation between numerical and experimental observations. This hybrid approach provides a more comprehensive understanding of cavitation behavior, revealing how variations in cavitation intensity and turbulence levels shape the acoustic signature of the pump, and offering deeper insight into cavitation dynamics under realistic operating conditions.

2. Methodology

(Model CRT 100-BR) operating with ISO 22 hydraulic oil at 40 °C, with a pump power of 1 HP and a system pressure of 6 bar. The system consists of polypropylene random copolymer (PPR) pipes with a suction diameter of 1.5 inches and a discharge diameter of 1.25 inches (connected via a reducer fitting), and a galvanized steel tank measuring 90 × 60 × 60 cm. Operating conditions are controlled using a variable frequency drive (AC drive), and data are collected through an ADQ unit and logged on a computer for detailed acoustic analysis. Acoustic emissions from cavitation were captured using a microphone sensor placed near the suction side and before conducting the acoustic measurements, the microphone sensor was calibrated to ensure the accuracy and reliability of the recorded sound pressure levels. A standardized sound level calibrator (SLC) was used to perform the calibration

The microphone was calibrated using a standard sound level calibrator providing 94 dB at 1 kHz. The microphone was fitted into the calibrator, and the corresponding output voltage was recorded. The sensitivity (mV/Pa) was calculated using the ratio of the measured voltage to the reference pressure (1 Pa). operating within −40 °C to +90 °C, Pressure transducers were installed at both suction and discharge sides, calibrated prior to the experiments with an accuracy of ±0.25%.

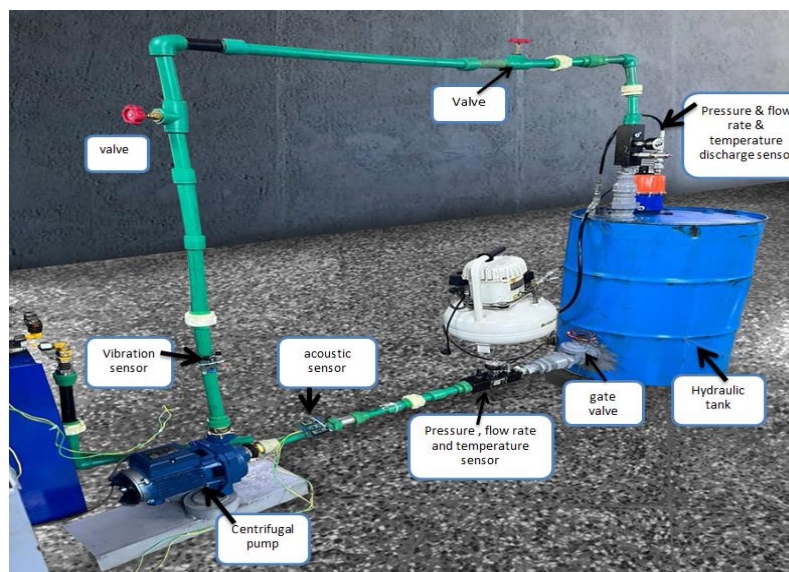


Fig. 1. The experimental setup

Table 1. Parameters of the working fluid

Parameter	Specification
Working fluid	Hydraulic oil ISO 22
viscosity $\mu/(\mu\text{Pa} \cdot \text{s})$ at 40c	20-24
Density $\rho/(\text{Kg/L})$	0.862
Vapour pressure at 40C	0.1 kpa
Viscosity (cSt at 100°C)	4.15

Additionally, the kinematic viscosity of the ISO 22 hydraulic oil was measured to ensure consistent fluid properties, which are essential for accurate cavitation analysis, as shown in Figure 2. This enables accurate and consistent outcomes, aligning with the criteria specified in Table 1.

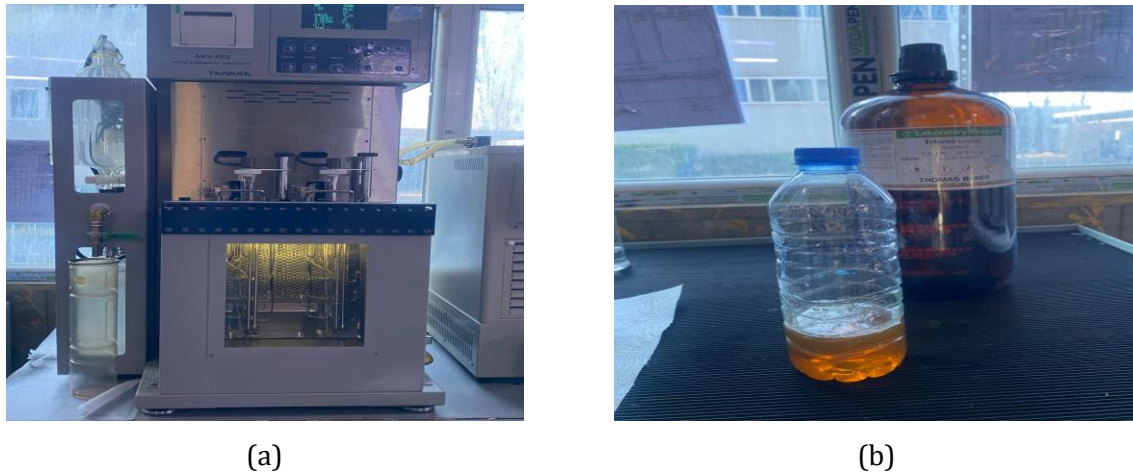


Fig. 2. (a) Automotive Kinematic Viscosity (AKV-202) and (b) Hydraulic iso 22

3. Numerical Simulation using CFX

CFX code is extensively utilized in the design, modeling, and resolution of various complicated industrial applications due to its high precision. CFX is commonly utilized to examine the distribution and regulation of flow variables in many industrial processes, including compressors, pumps, turbines, furnaces, boilers, hot rolling industries, and other applications where thermal management and mixing are essential. The optimization can facilitate substantial energy savings [15]. Employing CFX software facilitates the construction of a three-dimensional domain via computer technology. A computational mesh may subsequently be incorporated into this domain. [16].

To better understand internal flow dynamic many researches have relied on CFD technique as illustrated in the following studies, A. Al-Obaidi, et al. [17] conducted a CFD numerical simulation to investigate the impact of volute design on pump performance. Upon comparing the simulation results with the experimental data, it became evident that the outputs of both techniques were congruent. The pump head was shown to rise with the cross-sectional area of the pump volute. Pei et al. [18] utilized CFD technology to evaluate the influence of the impeller intake diameter D_1 , the inlet incidence angle $\Delta\beta$, and the blade twist angle φ on the cavitation performance of the centrifugal pump. To ascertain the optimal parameter settings for pump design, the cavitation features of the pump are analyzed utilizing orthogonal Design of Experiments (DOE). The internal flow of the enhanced impeller was analyzed and compared with that of the original flow. Ahmed R. Mahdi [19] carried out a CFD study to analyze the flow behavior and cavitation in a centrifugal pump under single-phase and cavitating conditions. He investigated the effect of different numbers of impeller blades on pressure, velocity, and vapor volume fraction. The results showed that cavitation started at the impeller eye and became more severe with fewer blades, especially at high flow rates. Wu et al. [20] used CFX software to analyze an enhanced cavitation model in CEL language, conducting numerical simulations of full flow under cavitation effects at three different temperatures: 25°C, 50°C, and 70°C, using an electronic water pump

The current study A three-dimensional numerical simulation of a centrifugal pump was conducted with ANSYS CFX software to examine the flow and identify cavitation. The diagram below delineates the process of preparing the numerical model, commencing with the design of the geometry and meshing, followed by. The $k-\omega$ turbulence model was used for its accuracy in near-wall flows, while cavitation was simulated using the Zwart-Gerber-Belamri (Rayleigh-Plesset-based) model to predict vapor formation and bubble dynamics for enhanced accuracy, and

concluding with the specification of boundary conditions, including inlet flow rate, rotational speed, and outlet pressure.

3.1 Geometry

The geometry of a centrifugal pump plays a crucial role in determining its internal fluid dynamics and cavitation behavior. In this study, a detailed 3D model of the pump was constructed, including all major components such as the inlet, outlet, impeller blades, and casing. Accurate dimensions were taken based on the proposed model, ensuring that the computational and experimental analyses reflect realistic flow behavior. The working fluid used in all simulations and experiments was an ISO VG 22 hydraulic oil. This geometric model, together with the specified fluid properties, was used in ANSYS CFX to study the pressure distribution, vapor volume fraction, and turbulent kinetic energy under various operating conditions. The key geometric parameters of the centrifugal pump, including the impeller and volute dimensions, were determined based on the manufacturer specifications and are summarized in Table 2. Figure 3 shows the geometry of the centrifugal pump

Table 2. Specification of the CRT-100 centrifugal pump prototype

Parameter	Value
Impeller outer diameter	92.40mm
Outlet pipe inner diameter	21mm
Volute width at outlet	71.47mm
Volute tongue length	25.27mm
Volute casing thickness	20.29mm
Pump rotation speed	2800rpm
Length of inlet pipe	0.5m
Length of outlet pipe	1m
Number of blades	8

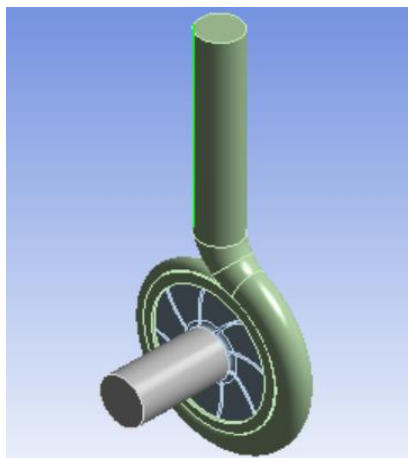


Fig. 3. Geometric of Centrifugal Pump

3.2 Meshing of the Flow

Partitions the domain into discrete elements or control volumes to numerically solve governing equations, is an essential aspect of computational analysis [15]. This study employed inflated layers at the fluid domain boundaries to precisely record the velocity and pressure gradients next to the wall surfaces. The pump geometry, including the inlet, impeller, and volute regions, was meshed using high-quality tetrahedral elements. Eight prismatic inflation layers were applied along all walls to improve near-wall resolution and accurately capture cavitation, pressure, and velocity gradients Figure 4(a). Mesh parameters included a transition ratio of 0.52 and a growth rate of 1.2, ensuring smooth refinement from coarse to fine regions. The global element size was 1.5 mm, with a finer 1.6 mm mesh for the impeller and volute to resolve high-gradient areas. The mesh comprised 451,099 nodes and 1,638,980 elements Figures 4(b) and mesh independence was

confirmed by minimal variations in output parameters. For boundary conditions, a flow rate was specified at the pump suction, while a static pressure was set at the discharge, and all other fluid interfaces were treated as non-slip walls to capture near-wall viscous effects. The inlet temperature was imposed to account for thermal influences on cavitation inception and vapor pressure variations of ISO VG 22 hydraulic oil as shown in figure 5 and table 3. Turbulence was modeled using the SST $k-\omega$ model, selected for its ability to accurately resolve adverse pressure gradients and flow separation within turbomachinery components. The study used an eight-blade impeller to enhance flow consistency and hydraulic performance under varying operating conditions.

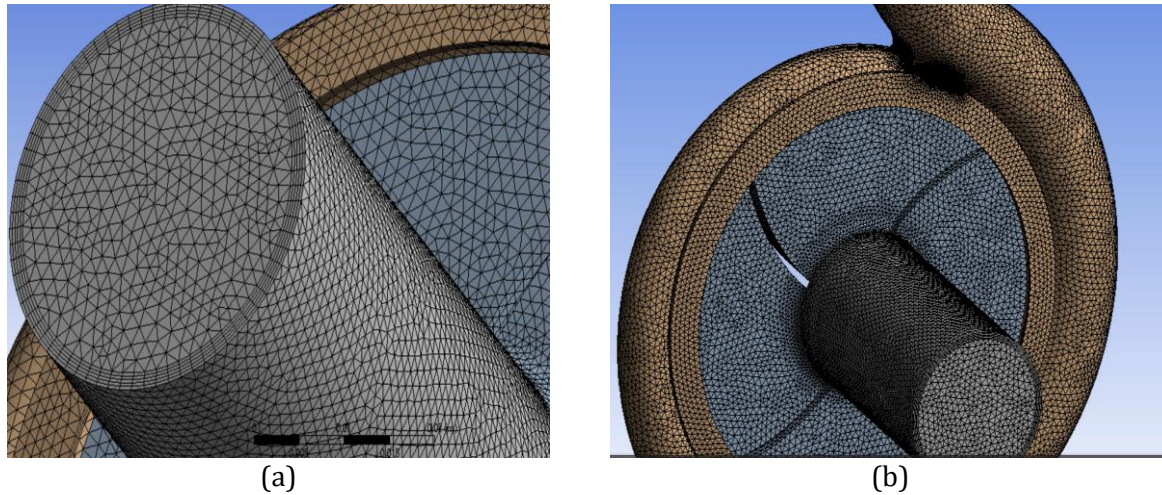


Fig. 4. (a) Inflation of the centrifugal pump and (b) meshing

A fixed static pressure outlet was applied to ensure stable convergence and to represent the actual discharge conditions of the pump. This boundary condition allows the flow rate to adjust naturally according to the pump's hydraulic performance, providing a physically realistic prediction of cavitation intensity and vapor distribution at the outlet.

Table 3. Specifications of operating conditions and material

Parameters	Value
Rotation speed	2800rpm
Flow rate	280 L/min
Head	20 m
Working fluid	Hydraulic oil iso 22
Vapor pressure at 40c	0.1 kpa
Density	0.862 (Kg/L)
Viscosity	24 $\mu/(\mu\text{Pa} \cdot \text{s})$ at 40c

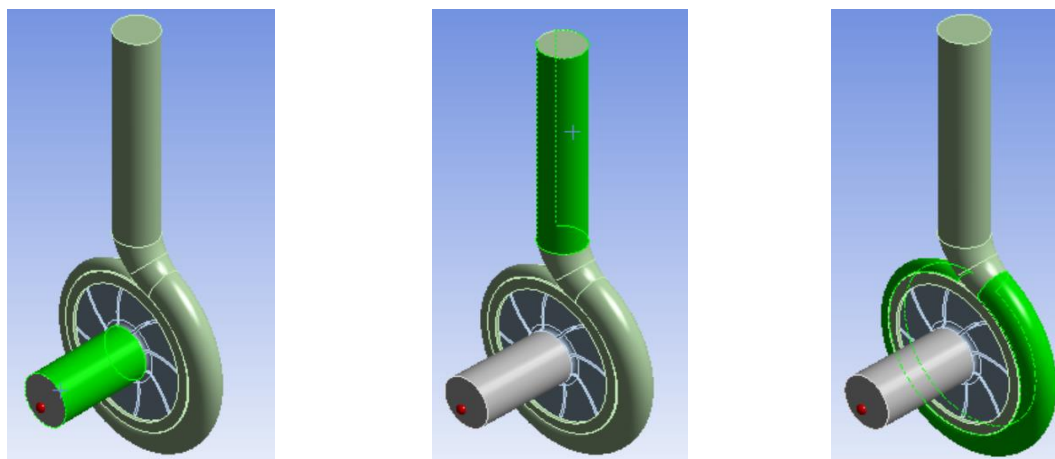


Fig. 5. Boundary condition, inlet, outlet and rotation

In the pre-processing stage, the computational domain was generated and discretized, and boundary conditions were applied. During the solution stage, the governing equations for continuity, momentum, and turbulence were solved iteratively up to a maximum of 500 iterations or until numerical convergence was achieved. A residual target of 10^{-4} was adopted as the convergence criterion, as shown in figure 6.

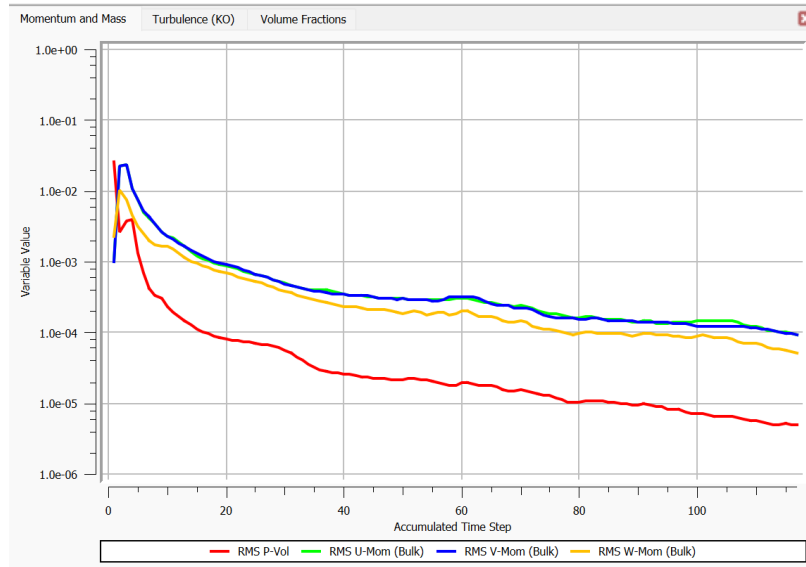


Fig. 6. Convergence in ANSYS CFX

4. Results and Discussion

4.1 Acoustic Techniques to Predict Cavitation in a Centrifugal Pump at Different Flow Rates

This study aimed to examine pump performance during standard operation and cavitation conditions by acoustic techniques. This approach requires certain sensors, such as a microphone, together with a dependable system for processing and analyzing signals to examine the acoustic signal associated with cavitation in a pump under various operating situations]

- Time Domain acoustic Signal: Initially, we compare the unprocessed acoustic signals under various operational settings with a time waveform analysis (TWFA) graph.
- To statistically assess the time-domain data acquired during the experiments or simulations, many common statistical parameters were utilized. These encompass the root mean square (RMS), peak to peak, and mean value. These metrics assess the amplitude, dispersion, and central tendency of the data temporally. [21]. The subsequent equations were utilized:
- Root Mean Square (RMS):

$$RMS = \sqrt{\frac{1}{N} \sum_{i=1}^N x_i^2} \tag{1}$$

Where N and x stand for the total number of elements and the element signal, respectively.

- Mean Value (μ):

$$\mu = \frac{1}{N} \sum_{i=0}^{N-1} x_i \tag{2}$$

The elements' mean values, their total number, and their set are represented by the variables x, xi and N.

- Peak-to-Peak Value:

$$P = x_{max} - x_{min} \tag{3}$$

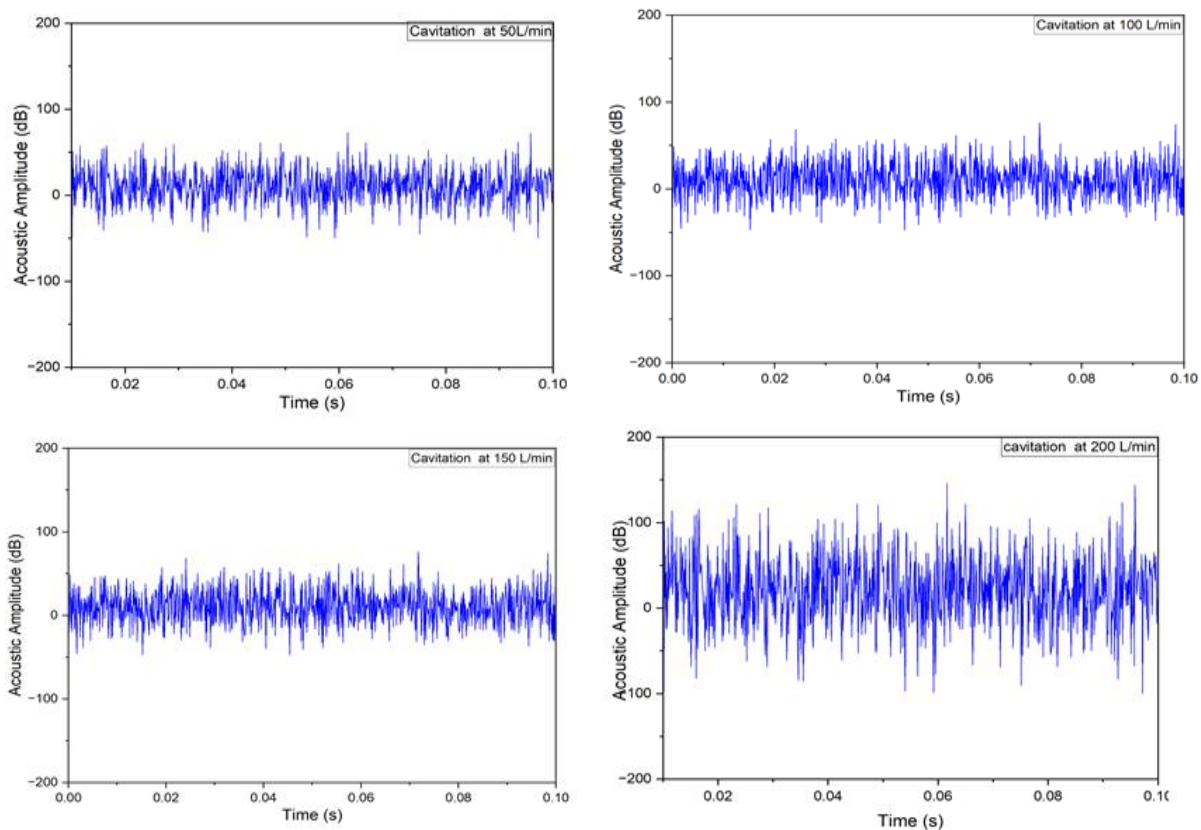
RMS, mean, and peak values were selected because they provide complementary insight into cavitation-induced acoustic behavior. The mean captures the overall signal level, the RMS reflects the effective energy content of the vibration or sound, and the peak value identifies extreme pressure fluctuations associated with bubble collapse. Together, these metrics offer a simple yet robust representation of cavitation intensity in the time domain.

These features were employed to discern several stages of cavitation within the pump (absence of cavitation, initiation of cavitation, and progression of cavitation). An acoustic sensor was employed to analyze sound pressure signals across various operating circumstances. The study's results were classified according to different flow rates, examining the duration and amplitude of the acoustic waveform signals at flow rates of 50, 100, 150, 200, 250, and 300 liters per minute, while maintaining a constant rotating speed of $N = 2800$ rpm. The results demonstrate that the amplitude of acoustic waves fluctuates with alterations in flow rate. For instance:

- At low flow rates (50–150 liters/min), the amplitude of the acoustic signal is very stable.
- At elevated flow rates (200–280 liters/min), the amplitude of the acoustic emissions starts to rise.

The research indicates that the amplitude of the acoustic signal escalates with an increase in flow rate, as shown in Figure 7. This phenomenon may be attributed to two primary factors: the contact between the impeller and the tongue area, and the initiation of cavitation at elevated flow rates, which intensifies with increasing flow (as shown in Figure 6). Under these circumstances, the acoustic signal patterns became increasingly erratic and had elevated peaks relative to standard operating settings.

Utilizing many statistical metrics reflecting vibration in the time domain, including peak, RMS, and mean characteristics. These properties provide a valuable resource, and often utilized in condition monitoring. Figure 8 demonstrates that the peak feature value was more effective in detecting cavitation based on signal energy content compared to the RMS and mean features. The Peak-to-Peak vibration signal was roughly 42.86% more than the RMS signal as shown in table 4, suggesting that Peak to Peak is more adept at detecting changes related to cavitation within this flow range. And figure 9 shown the Peak Acoustic Amplitude Levels Under Two Operational Conditions



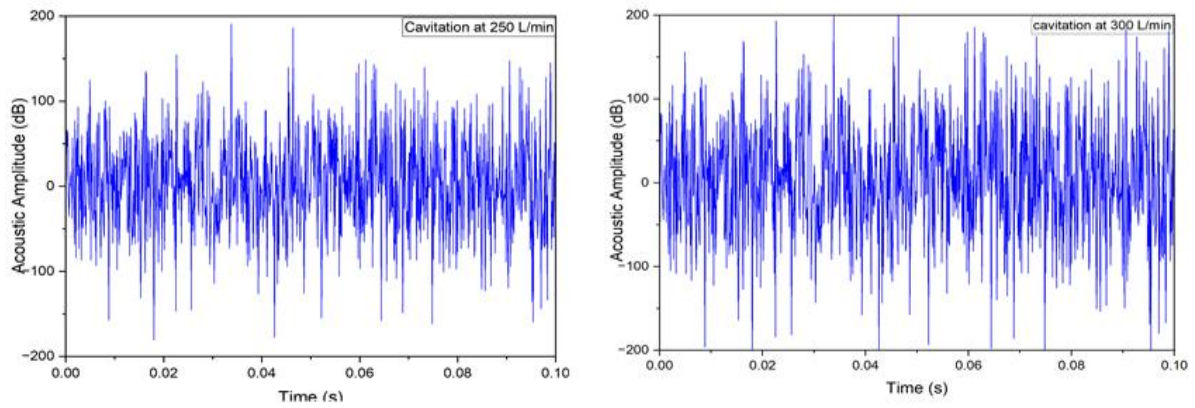


Fig. 7. Acoustic signal at different flow rate at 2800 rpm

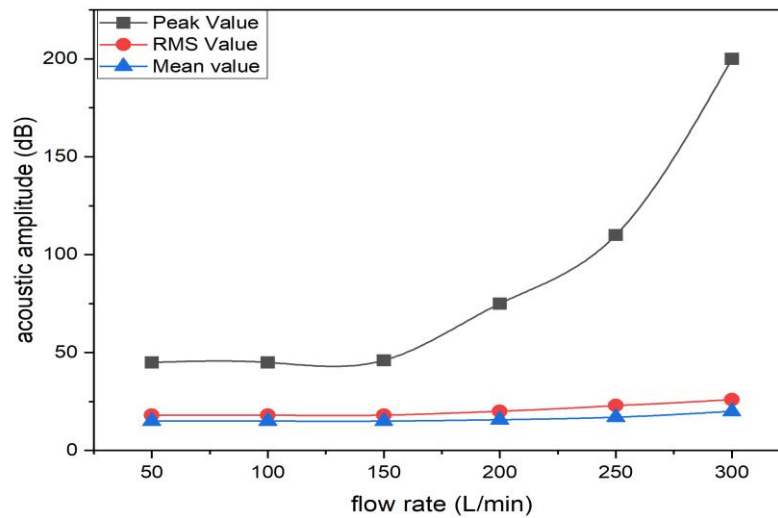


Fig. 8. Acoustic signal's (Peak to Peak, Mean and RMS) at 2800 rpm

Table 4. Acoustic response (Peak/RMS/Mean) under varying flow rate conditions

Flow Rate (L/min)	Peak Value (dB)	RMS Value (dB)	Mean Value (dB)
50	45	17	15
100	46	17	15
150	44	17	15
200	60	18	16
250	110	20	17
300	200	22	19

Pump housing vibrations can superimpose structural noise onto the acoustic measurements, potentially increasing RMS and peak levels. Mechanical vibrations from motor, bearings, or flow-induced forces may excite the housing, transmitting additional signals to the microphone. Careful sensor placement, vibration isolation, and signal filtering are necessary to ensure that the measured acoustic signals primarily reflect cavitation phenomena rather than structural vibrations.

4.2 Simulation

This section presents the results of the simulations conducted in ANSYS CFX for a centrifugal hydraulic pump under various flow rates. Cavitation detection was carried out by calculating the vapor volume fraction and turbulence kinetic energy.

4.2.1 Vapor Volume Fraction Contour in The Centrifugal Hydraulic Pump

This paragraph analyzes the distribution of vapor volume fraction during cavitation to evaluate the initiation and development of cavitation inside the internal flow regions of a centrifugal pump at different flow rates. Figure 8 illustrates the distribution of vapor volume % at the impeller intake at various flow rates. The vapor volume fraction was also evaluated to assess cavitation occurrence within the hydraulic centrifugal pump. As shown in the contour plots and the accompanying graph, there is a clear increase in vapor volume at flow rates beyond 150 L/min, with a significant surge observed at 250 and 300 L/min. An increase in the flow rate from 200 L/min to 300 L/min led to a 45% rise in the vapor volume fraction. The sudden rise in vapor fraction above 200 L/min is caused by local pressure dropping below the fluid's vapor pressure due to higher flow velocities. As the flow rate increases, the centrifugal pump suction region experiences stronger acceleration and turbulence, lowering static pressure and promoting rapid bubble formation. This process is amplified by turbulence-induced fluctuations, which enhance cavitation growth and lead to a sharp increase in vapor volume fraction. This indicates the formation and growth of vapor bubbles due to local pressure drops below the fluid's vapor pressure a key characteristic of cavitation.

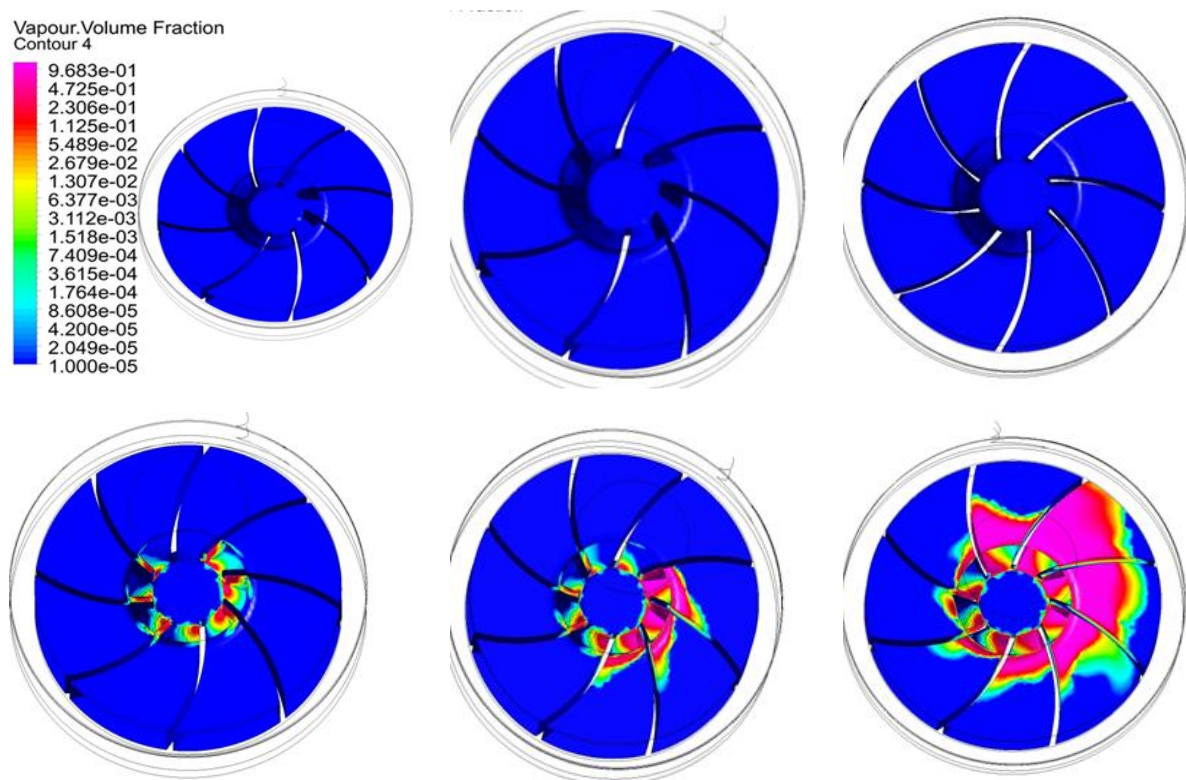


Fig. 9. Vapor volume fractions contour under different flow rates at 2800 rpm

4.2.2 Turbulent Kinetic Energy in The Centrifugal Hydraulic Pump

Turbulent kinetic energy (TKE) is crucial for comprehending the internal flow dynamics of hydraulic centrifugal pumps. It indicates the severity of turbulence produced when the fluid traverses important areas, including the impeller and volute casing. Examining TKE yields significant insights on flow instability, energy dissipation, and the likelihood of cavitation. This research assessed TKE at flow rates between 50 and 300 L/min, maintaining a constant rotating speed of 2800 rpm. The contour plots show that at low flow rates (50–150 L/min), the turbulence remains relatively low and localized, primarily around the impeller. As the flow rate exceeds 200 L/min, turbulence intensifies and becomes more broadly dispersed throughout the volute and blade channels. The graph depicting average TKE in relation to flow rate substantiates this trend: TKE diminishes little from 50 to 150 L/min, thereafter experiences a substantial increase, peaking at 300 L/min. Increasing the flow rate from 200 L/min to 300 L/min resulted in a 65% increase in turbulent kinetic energy. The fast escalation of turbulence at elevated flow rates signifies increasing

flow instability and the possible emergence of cavitation, particularly in high-velocity areas next to the blade trailing edges and volute tongue. The results indicate a significant association between flow rate and turbulence development, underscoring the usefulness of TKE analysis in forecasting unstable circumstances and enhancing pump performance, as shown in Figure 10.

Turbulence affects the acoustic signature by modulating pressure fluctuations within the pump. Higher turbulence intensity increases chaotic, high-frequency flow structures, which generate stronger and more irregular acoustic emissions. These fluctuations enhance noise amplitude (RMS and peak) and alter the spectral content, making it possible to correlate specific turbulence patterns with cavitation intensity and bubble collapse events.

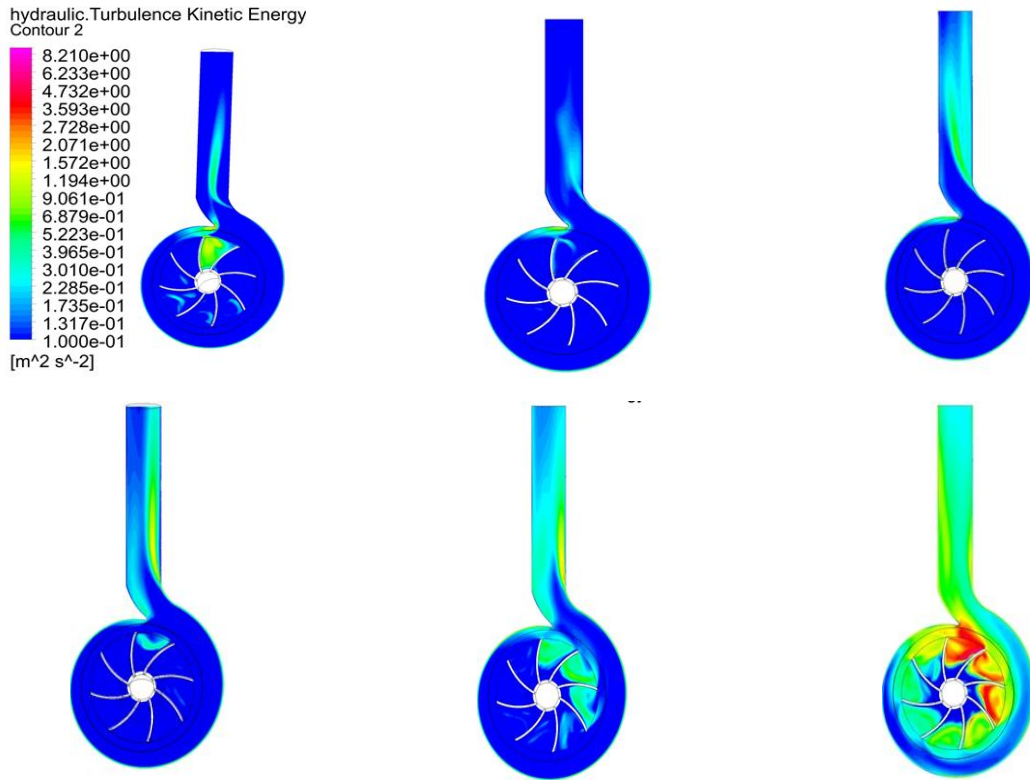
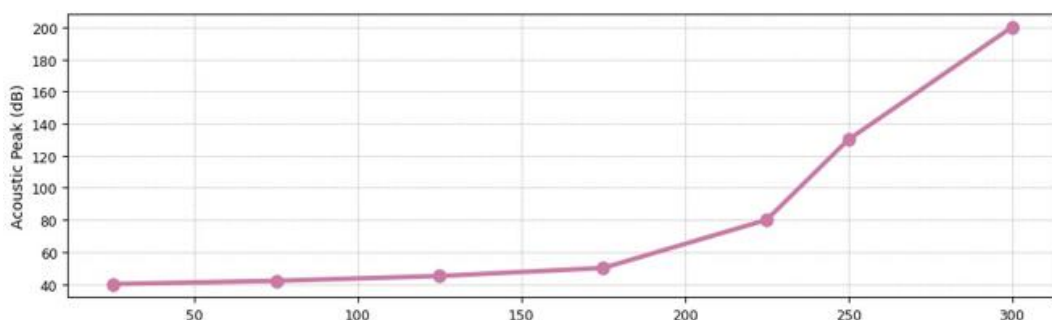


Fig. 10. Turbulence kinetic energy contour at different flow rate at 2800 rpm

4.3 Validation

The vapour volume fraction, turbulent kinetic energy, and acoustic emissions are key indicators of cavitation in centrifugal pumps, each reflecting a different physical aspect of the phenomenon. The vapour volume fraction indicates the amount of vapor bubbles formed due to pressure drop, while turbulent kinetic energy (TKE) reflects the intensity of flow disturbances caused by these bubbles. The acoustic signal represents the noise generated by their collapse on the impeller surfaces. Notably, at the same flow rates, both the vapors volume fraction and sound levels increased simultaneously, confirming a direct link between the growth of vapor bubbles and the corresponding rise in acoustic emissions during cavitation, as shown in figure 11.



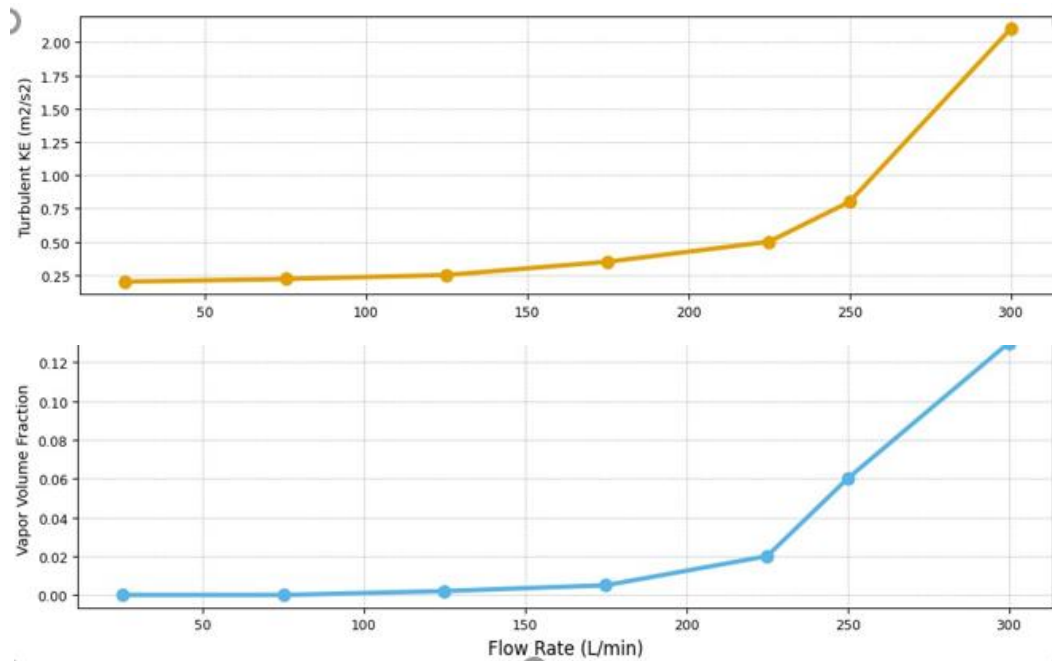


Fig. 11. Experimental and CFX parameters with flow rate for cavitation detection

5. Conclusion

Centrifugal pumps play a critical role in fluid transmission, particularly in hydraulic systems requiring high flow rates and pressures. Understanding the factors that influence their performance, such as rotational speed and fluid properties, is essential for enhancing efficiency and mitigating issues like cavitation. Advances in acoustic analysis and other diagnostic techniques are vital for ensuring reliable and economical hydraulic system operation. The current study combining ANSYS CFX simulations with experimental acoustic measurements effectively captures cavitation behavior in a CRT 100-BR centrifugal pump using ISO 22 hydraulic oil. Results showed that cavitation initiates above 150 L/min, with sharp increases in vapor volume fraction and turbulent kinetic energy at higher flow rates, particularly above 200 L/min. Corresponding acoustic signals reflected these changes, with peak amplitudes about 43% higher than RMS values, confirming the sensor's sensitivity to cavitation. These findings highlight the practical value of integrating numerical and acoustic analyses for pump condition monitoring. Limitations include the use of a single fluid type and flow configuration, suggesting that further studies under varied operating conditions would strengthen generalization.

References

- [1] Mousmoulis G, Anagnostopoulos J, Papantonis D. A review of experimental detection methods of cavitation in centrifugal pumps and inducers. *Int J Fluid Mach Syst.* 2019;12(1):71-88. <https://doi.org/10.5293/IJFMS.2019.12.1.071>
- [2] Wu P, Bai L, Lin W, Wang X. Mechanism and dynamics of hydrodynamic-acoustic cavitation (HAC). *Ultrason Sonochem.* 2018;49:89-96. <https://doi.org/10.1016/j.ultsonch.2018.07.021>
- [3] Gu Y, et al. Suppression of unsteady partial cavitation by a bionic jet. *Int J Multiph Flow.* 2023;164:104466. <https://doi.org/10.1016/j.ijmultiphaseflow.2023.104466>
- [4] Černetič J, Čudina M. Cavitation noise phenomena in centrifugal pumps. In: 5th Congress of Alps-Adria; 2012. p. 1-6.
- [5] Farokhzad S, Ahmadi H. Acoustic based cavitation detection of centrifugal pump by neural network. *J Mech Eng Technol.* 2013;1(1):1-5. <https://doi.org/10.18005/JMET0101001>
- [6] Hosien MA, Selim SM. Acoustic detection of cavitation inception. *J Appl Fluid Mech.* 2017;10(1):31-40. <https://doi.org/10.18869/acadpub.jafm.73.238.25638>
- [7] Dong L, Zhao Y, Dai C. Detection of inception cavitation in centrifugal pump by fluid-borne noise diagnostic. *Shock Vib.* 2019;2019(1):9641478. <https://doi.org/10.1155/2019/9641478>

- [8] Ranade NV, Sarvothaman V, Ranade VV. Acoustic analysis of vortex-based cavitation devices: Inception and extent of cavitation. *Ind Eng Chem Res.* 2021;60(22):8255-8268. <https://doi.org/10.1021/acs.iecr.1c01005>
- [9] Al-Obaidi AR. Experimental diagnostic of cavitation flow in the centrifugal pump under various impeller speeds based on acoustic analysis method. *Arch Acoust.* 2023;48(2):159-170. <https://doi.org/10.24425/aaa.2023.145234>
- [10] Karagiovanidis M, Pantazi XE, Papamichail D, Fragos V. Early detection of cavitation in centrifugal pumps using low-cost vibration and sound sensors. *Agriculture.* 2023;13(8):1544. <https://doi.org/10.3390/agriculture13081544>
- [11] Stephen C, Basu B, McNabola A. Detection of cavitation in a centrifugal pump-as-turbine using time-domain-based analysis of vibration signals. *Energies.* 2024;17(11):2598. <https://doi.org/10.3390/en17112598>
- [12] Ajmi RE, Hussein HA, Numan AH. Experimental investigation of inception cavitation phenomena effect in centrifugal pumps using hydrophone sensor. *JJMIE.* 2025;19(1). <https://doi.org/10.59038/jjmie/190110>
- [13] Ni C, Zhang D, Shen X, Xu B, Lang T, Gao X. Cavitation-induced vibration and noise signal analysis of a single blade centrifugal pump. *Phys Fluids.* 2025;37(8). <https://doi.org/10.1063/5.0283743>
- [14] Wang D, Ma W, Zhao W, Cao R, Yang Y. Experimental acoustic analysis of cavitation in a centrifugal pump. *Fluid Dyn Mater Process.* 2025;21(4). <https://doi.org/10.32604/fdmp.2024.055220>
- [15] Hosain ML, Fdhila RB. Literature review of accelerated CFD simulation methods towards online application. *Energy Procedia.* 2015;75:3307-3314. <https://doi.org/10.1016/j.egypro.2015.07.714>
- [16] Jaiswal NP. CFD analysis of centrifugal pump: a review. *J Eng Res Appl.* 2014;4:175-178.
- [17] Al-Obaidi A, Pradhan S, Asim T, Mishra R, Zala K. Numerical studies of the velocity distribution within the volute of a centrifugal pump. 2014.
- [18] Pei J, Yin T, Yuan S, Wang W, Wang J. Cavitation optimization for a centrifugal pump impeller by using orthogonal design of experiment. *Chinese J Mech Eng.* 2017;30(1):103-109. <https://doi.org/10.3901/CJME.2016.1024.125>
- [19] Al-Obaidi AR. Monitoring the performance of centrifugal pump under single-phase and cavitation condition: A CFD analysis of the number of impeller blades. *J Appl Fluid Mech.* 2019;12(2):445-459. <https://doi.org/10.29252/jafm.12.02.29303>
- [20] Wu K, Ali A, Feng C, Si Q, Chen Q, Shen C. Numerical study on the cavitation characteristics of micro automotive electronic pumps under thermodynamic effect. *Micromachines.* 2022;13(7):1063. <https://doi.org/10.3390/mi13071063>
- [21] Proakis JG. Digital signal processing: principles algorithms and applications. India: Pearson Education India; 2001.